

## Mixed Oxides for Photo-electrochemical Applications

Pablo Ampudia<sup>\*a</sup>, Simonetta Palmas<sup>a</sup>, Annalisa Vacca<sup>a</sup>, Michele Mascia<sup>a</sup>, Laura Mais<sup>a</sup> and Frank Marken<sup>b</sup>

<sup>a</sup>Dipartimento di Ingegneria Meccanica Chimica e dei Materiali, Università degli Studi di Cagliari. Via Marengo 2, 09123 Cagliari, Italy

<sup>b</sup>Department of Chemistry, University of Bath, Bath BA2 7AY, UK  
 p.ampudia@dimcm.unica.it

The photoexcitation of an n-type photo-anode and a p-type photo-cathode provides electrons and holes in photo-electrochemical processes. Depending on the use of photosensitive material as anode, cathode or both, different photo-electrochemical (PEC) system configurations and experimental conditions have to be taken into account to consider "green" the photo-electrochemical process when solar energy and water are used to drive the process. Several studies have been done by our group in order to obtain a photo-anode driven PEC cell in which a lowering of the applied cell voltage was obtained from the photo-potential generated at TiO<sub>2</sub> nanotubular structures. Among other p-type semiconductors, Ni oxides based photo-cathodes, coupled to different photo-anodes are proposed in the literature as inexpensive semiconductors in photo-catalysis. However, the absorption spectrum of these metal oxides is limited to ultraviolet region due to their large band gap and therefore efforts to activate Ni oxide and TiO<sub>2</sub> for a visible light range have to be done. In particular, the literature proposed the combination of different electronic structures, based on mixed metal oxide photo-catalysts to enhance the light-response range to the visible region, thereby promoting the photo-catalytic efficiency.

The present work proposes the synthesis of hierarchical structures of Ti/Al and Ni/Al mixed oxides. TiO<sub>2</sub> nanotubular structures were obtained by oxidation of a Ti foil in deionized water and glycerol organic solution with NH<sub>4</sub>F at room temperature. Ni oxide films were obtained supported onto Indium Tin Oxide (ITO) coated glass. Doctor-blade method and subsequent annealing treatment were adopted to obtain a stable structure. Commercially available Nickel oxide nanopowders and nanowires were used, as well as alcoholic solution of nickel-nitrate salt, all dissolved into N,N-dimethylformamide (DMF) were used as precursor solutions to obtain home-made Ni oxide. Aluminum oxide, embedded in the Ni oxide and Ti oxide structures by repeated dipping/thermal cycles, is proposed to enhance the photo-catalytic performance of the bare Ti and Ni oxides.

The materials were morphologically and electrochemically characterized by scanning electron microscopy, cyclic voltammetry and chrono-amperometry analysis. The stability and photo-catalytic activity of the synthesized samples were studied.

### 1. Introduction

Photo-electrocatalysis is a potential application for photosensitive metal oxide semiconductor materials. A green process can be afforded by using these materials in PEC systems, thanks to their high efficiency in absorbing sunlight, so creating delocalized charges, and producing electrical current. However, the main drawback of these materials is represented by the rapid recombination between the photo-generated electron-hole pairs. So, the development of photosensitive nanostructured materials at which the recombination is reduced is a topic of great interest.

Titanium dioxide (TiO<sub>2</sub>) is widely used in PEC systems as n-type photo-catalytic anodic material, due to its optical and electronic properties, as well as its low cost, environmental compatibility, high activity and large stability. Parallely, when cathodic materials are considered, p-type oxide semiconductors have become an active area of research (Castillo et al., 2015; D'Amario et al., 2014). Both the solutions may represent a way to reduce the cell overvoltage of the PEC. Several studies are reported in the literature in which different Nickel

oxide (NiO) based photo-cathodes are proposed as efficient p-type oxide semiconductors to replace the common counter electrode used in conventional PEC.

However, due to their large bandgaps (3.2eV and 3.6eV, respectively), the absorption spectrum of TiO<sub>2</sub> and NiO is limited to ultraviolet region, which accounts for only a small fraction (<5%) of the incoming solar light. In this context, visible-light driven photo-catalysts should be developed to enhance the photo-catalytic activity of these materials in solar energy conversion processes.

Compared to single phase photo-catalysts, heteronanostructured mixed metal oxides can enhance the light-response range to the visible region and improve the charge separation and transfer properties, thus promoting the photo-catalytic efficiency (Li et al., 2013). According to Hu et al. (2014), the addition of Al<sub>2</sub>O<sub>3</sub> blocking layer to NiO photocathodes, fabricated by alkaline etching-anodizing of nickel foils, minimizes surface charge recombination on the NiO and increases the incident photon-to-current conversion efficiency. Moreover, enhancement of the visible-light photocatalytic activity of TiO<sub>2</sub> is reported in the literature when N-doped P25 TiO<sub>2</sub> is combined with amorphous Al<sub>2</sub>O<sub>3</sub> prepared via one-step solution combustion method (Li et al., 2012).

In this paper, we propose the synthesis of hierarchical structures in which Al oxide is embedded in Ti oxides and Ni oxides to enhance the photo-catalytic activity of the single oxide phases, in the range of the near visible light, for PEC applications. Results on the oxidation of glycerol are also reported to assess the effectiveness of Ti/Al mixed oxide structures in oxidizing organic substrates.

## 2. Experimental procedures

### 2.1 Synthesis of Ti/Al and Ni/Al mixed oxides

TiO<sub>2</sub> nanotubular structured samples (T1) were obtained by electrochemical oxidation of Ti foils according to a procedure described in previous work (Palmas et al., 2014).

Ni oxide nanoporous substrates were obtained supported onto Indium Tin Oxide (ITO) coated glass. To this aim, slides of ITO were sonicated 30 min in acetone, washed in distilled water and heated for 1 h at 500 °C. Depending on the samples, commercially available Nickel oxide nanopowders (NP) and nanowires (NW), as well as alcoholic solution of nickel-nitrate salt, all dissolved into N,N-dimethylformamide (DMF) were used as precursor solutions (PS) to obtain home-made Ni oxide. Table 1 shows the composition of the PS used to obtain the films. In one case (sample N4), a solution of a Polymer of Intrinsic Microporosity (PIM-1) dissolved in Chloroform (CHCl<sub>3</sub>) (1mg PIM-x/1 mL CHCl<sub>3</sub>) was added to the Ni oxide PS (Ratio 1 mL: 1 mL).

The doctor-blade method was adopted to obtain stable structures onto ITO substrates. All mixtures were treated in an ultrasonic bath for 30 min before being used. Then, 25 µL of PS were distributed onto 1cm<sup>2</sup> of the ITO substrate and dried at 100 °C in air for 10 min. To increase the thickness of the film, this process was repeated eight times for each sample. Finally, the samples were submitted to a thermal treatment at 500 °C for 1 h in air atmosphere in a tube furnace.

*Table 1: Composition of the Ni oxide PS; NP: 99.8% Nickel (II) Oxide nanopowder (A.P.S. <50 nm); NW: NiO nanowires; DMF: N,N-Dimethylformamide.*

Sample	Precursor Solution Composition
N1	0.06M of NiO NP in DMF
N2	0.06M of NiO NW in DMF
N3	0.06M of Ni(NO <sub>3</sub> ) <sub>2</sub> *6H <sub>2</sub> O in DMF
N4	0.06M of Ni(NO <sub>3</sub> ) <sub>2</sub> *6H <sub>2</sub> O in DMF containing the PIM-1 solution

Al oxide was embedded in the Ti and Ni oxide structures by dipping (20 min) the prepared samples in a 0.15 M Al-tri-sec-butoxide (1.0M in Dichloromethane), dissolved in 2-propanol solution. The Al solution was pre-heated at 65 °C prior the dipping. Finally, the samples were submitted to a thermal treatment at 435 °C for 20 min in air atmosphere (Palomares et al., 2003).

Just one dipping process was sufficient in the case of TiO<sub>2</sub> substrate, while in the case of Ni oxide substrate, previous investigation showed that the best performance could be obtained when this procedure was repeated six times. For simplicity, in the rest of the text the final hierarchical structures will be named as T1A for the Ti/Al sample, and N1A, N2A, N3A and N4A for the Ni/Al samples.

### 2.2 Experimental Methods

The electrochemical and photo-electrochemical experiments, as well as the characterization of all the samples were performed in a three electrode cell: the synthesized materials were used as working electrodes, while Platinum constituted the counter electrode. A saturated calomel electrode (SCE) was used as reference; all the potentials in the text are referred to it. Different oxo-acidic salt based aqueous solutions were used as

supporting electrolytes. In some experiments, a fixed amount of glycerol (30 %) was added to the electrolyte, to study the capability of the Ti/Al samples to oxidize organic compounds at different pH values.

Chronoamperometry tests were performed at different potential. For the experiments performed with the Ni/Al films, a high-power blue LED ( $\lambda=400\text{nm}$ , M405L2 UV LED, Thorlabs, Ely, UK) together with LED driver (T-Cube LED driver, Thorlabs, Ely, UK) and a DDS Function/Arbitrary TG4001 Generator (TTi, Huntingdon, UK) to regulate pulse frequency and intensity were employed. The light chopping frequency was set at 0.1 Hz and the experiments were performed by illuminating the films from the non-active side.

The photo-activity of Ti/Al oxide samples, was tested under a light flux provided by a 300W Xe lamp (Lot Oriel) equipped with an IR water-filter. Suitable optical filters were used in order to select different wave lengths of the incident light.

For all the cases, the photocurrent was calculated by subtracting the stable values measured in the dark from those obtained under irradiation. Cyclic Voltammeteries (CVs) were performed in the absence of light. Film morphology of the assembled electrodes was characterized by means of Scanning electron microscopy (JEOL JSM6301F and Zeiss Supra 40 FEG-SEM).

### 3. Results and Discussion

#### 3.1 Morphological and electrochemical characterization

Previous work carried out in our laboratory allowed to individuate a simple synthesis method to obtain regular and stable nanotubular (NT) structures of  $\text{TiO}_2$ , starting from Ti foils. An example of the morphology of the NT samples is shown in Figure 1a: a well defined  $\text{TiO}_2$  NT structure is obtained with average pore diameter value of about 75 nm. Figure 1b shows voltammetric behavior of the sample: the repeated cycles of CV demonstrate its stability in aqueous solution. The effect of the modification of the electrode surface by the Al-oxide is highlighted in Figure 1c: a slight decrease in the current peak is observed in the cathodic as well as in the anodic regions (inset in Figure 1c).

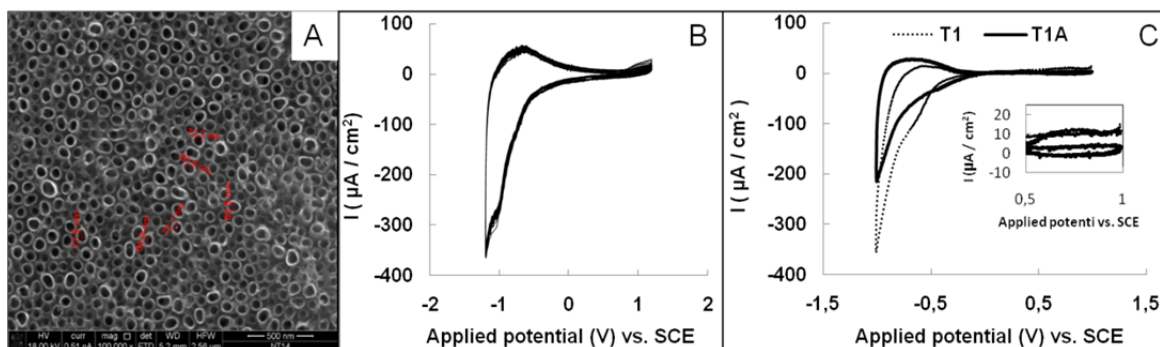


Figure 1: SEM images of the  $\text{TiO}_2$  NT structures (a); Repeated cycles of CV performed at T1 electrode (b) and (c) voltammograms obtained at T1 and T1A electrodes in 0.1 M  $\text{KNO}_3$  in the dark (scan rate:  $100\text{ mVs}^{-1}$ ).

If Ni based samples are considered, different types of solvent were tested in order to obtain stable Ni oxide substrates supported onto ITO. Among others, DMF resulted to improve the adhesion between the Ni oxide film and ITO substrate. Figure 2 shows an example of the CV obtained at these samples: the cycling in aqueous electrolyte has no significant effect on the oxide stability. Moreover, no flattening of the voltammograms, after fifty cycles, was observed, confirming the stability of the metal oxide to degradation or other possible phenomena.

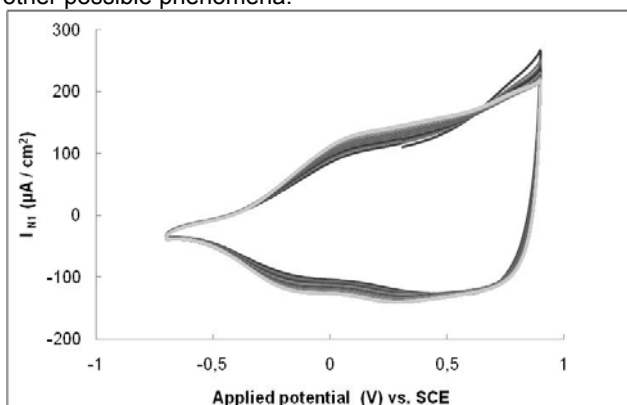


Figure 2: Repeated cycles of CV performed at N1 electrode in  $\text{Na}_2\text{SO}_4$  in the dark (scan rate:  $20\text{ mVs}^{-1}$ ).

The morphology of the Ni based samples is resumed in Figure 3. In particular, for sample constituted by commercial Ni nano-particulated oxide, a NiO layer, which appears aggregated into particles of several micron diameter is obtained (N1 sample). Nanowires structure, forming a more or less compact mesh, is characteristic of the N2 sample. When Ni oxide is obtained from the related salt (N3 and N4 samples) a structure of microspheres consisting of interconnected nanoplates is obtained. As it can be observed in Figure 3d, the use of PIM-1 generates nanostructures of smaller dimensions (N4).

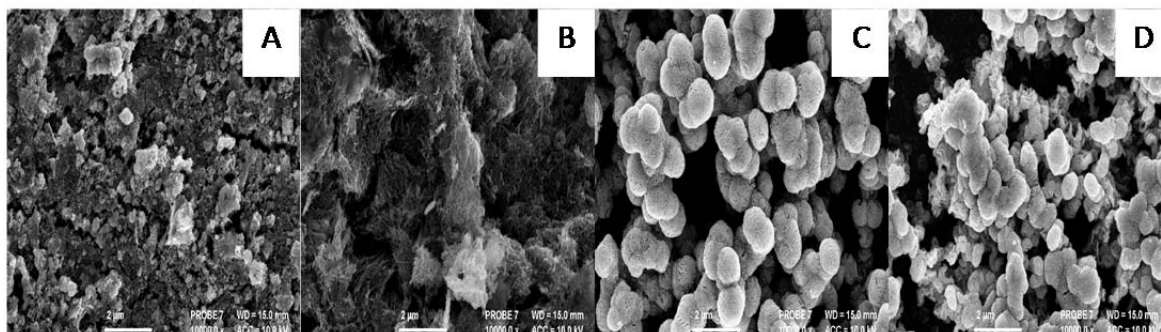


Figure 3: SEM images of the Ni oxide films: N1 (a), N2 (b), N3 (c) and (d) N4.

A comparison between the voltammograms obtained at the bare and hierarchical electrodes is reported in Figures 4a and 4b. Among all the Ni oxides, N1 and N2 films, obtained from commercial nickel oxide NP or NW, show higher capacitive behaviour which could be attributed to their relative small nanoparticle sizes. When Ni oxide is derived from the relevant salt solution (N3 and N4 samples) lower capacitance are obtained. In any case, the voltammetric area is lowered by the modification of the surface by the Al-oxide film.

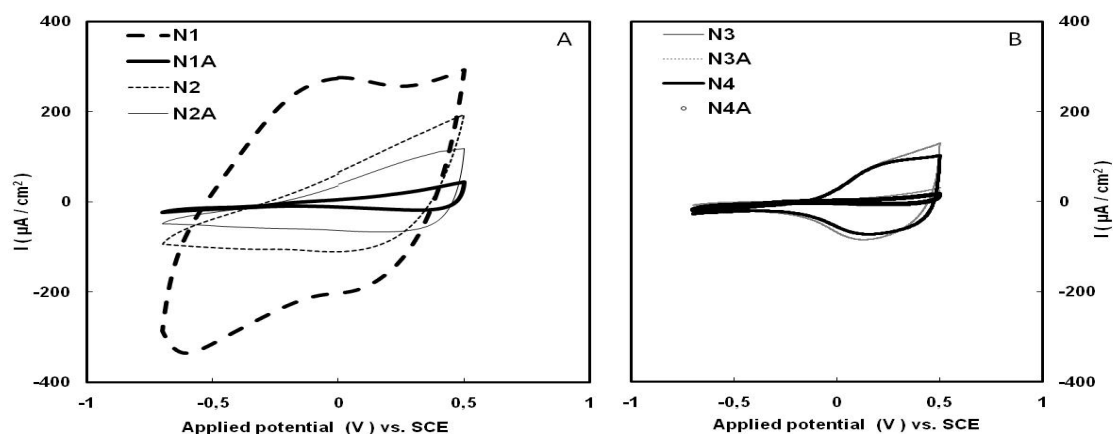


Figure 4: Voltammograms obtained at the N1, N1A, N2 and N2A (a) and (b) N3, N3A, N4 and N4A electrodes in 0.1M Na<sub>2</sub>SO<sub>4</sub> in the dark (scan rate: 20 mVs<sup>-1</sup>)

### 3.2. Photoelectrochemical characterization

The photoelectrochemical properties of all the synthesized electrodes, in the presence and in absence of Al oxide, are investigated in aqueous solution under chopped light conditions. The current scans were performed under different overpotentials from the open circuit voltage (OCV) of each sample.

In the case of the Ti based samples, the photocurrents of the Ti and Ti/Al oxide based electrodes were evaluated in aqueous KNO<sub>3</sub> solution under potential values at which the space charge of the semiconductor is in accumulation regime. Figure 5 shows the current trend, for both the electrodes, at different wavelength values ( $\lambda=365$  nm and  $\lambda=400$  nm).

As expected, (considering that the wide band gap for TiO<sub>2</sub> limits the light absorption within the UV wavelengths) higher absolute values of photocurrent were obtained at 365 nm (Figure 5a). Working at this wavelength, moderate gains in the photocatalytic behavior (if compared with bare electrode) are observed. However, at 400 nm, the Al oxide improves the performance of the bare TiO<sub>2</sub> based sample (T1A sample in Figure 5b). Actually, as shown in the figure, according to the voltammetric behaviour, the current recorded in the dark is lowered by the presence of the Al oxide, however the photocurrent is increased.

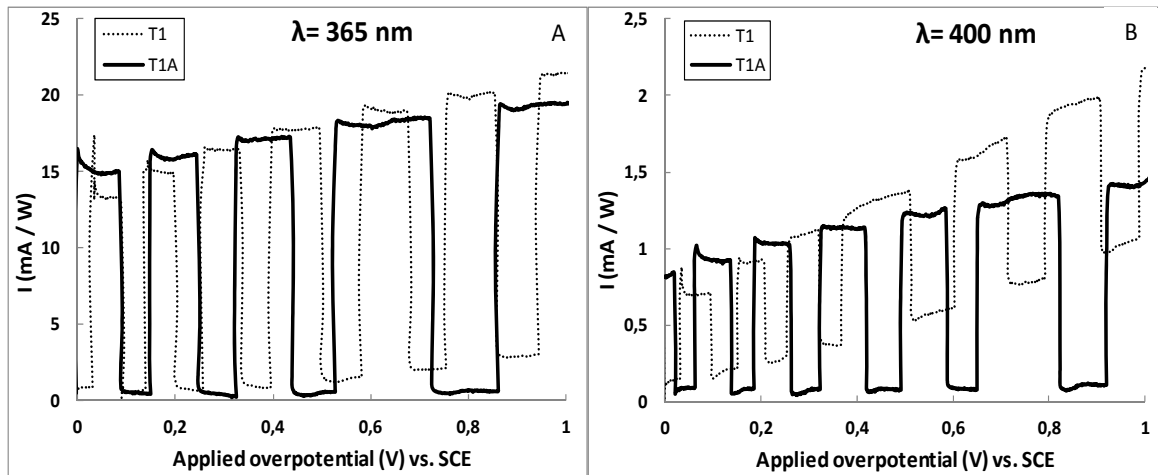


Figure 5: Normalized Photocurrent of T1 sample and T1A at 365 nm (a) and (b) 400 nm under chopped light irradiation in 0.1 M  $\text{KNO}_3$ .

In order to quantify the results, the photocurrent profit (PP) of the T1A sample, was calculated at 0.5 V of overpotential by the following equation:

$$PP = \frac{I_{xA}}{I_x} \quad (1)$$

where  $I_{xA}$  and  $I_x$  represent the normalized photocurrent values obtained from the experiments in which Al modified hierarchical structures or bare samples were used as working electrodes, respectively. The subscript "x", in equation (1), represents the type of synthesized electrode used for the calculation of the PP value.

The highest PP value (1.43), is obtained at 400nm while lower PP (1.08) is obtained at 365 nm.

As the Ni/Al oxides are considered, Figure 6 reports the values of photocurrent measured at 400 nm, and under 0.5 V of overpotential, in aqueous solution for the different Ni oxide samples. As it can be observed, except for N2 sample, the Al oxide has a positive effect on the photo-current. The different morphology of the mesh of NiO nanowires, may be assumed as responsible for the different behaviour obtained at this sample.

The highest photocurrent ( $5 \mu\text{A}/\text{cm}^2$ ) is recorded at N1A sample. However, it is worth to be noticed that high gains in the performance (if compared with bare electrodes) are obtained at the other samples, even if lower absolute values of photocurrents are measured. As an example, a PP value of 29.48 is obtained for the N3 sample when Al oxide is embedded in the structure. Hu et al. (2014) reported similar performances for NiO electrodes used for hydrogen production in PEC, when  $\text{Al}_2\text{O}_3$  is added. The positive effect of  $\text{Al}_2\text{O}_3$  which acts as tunnelling barrier that suppresses the back recombination of the photo-electrons at the NiO surface, was assessed from the authors.

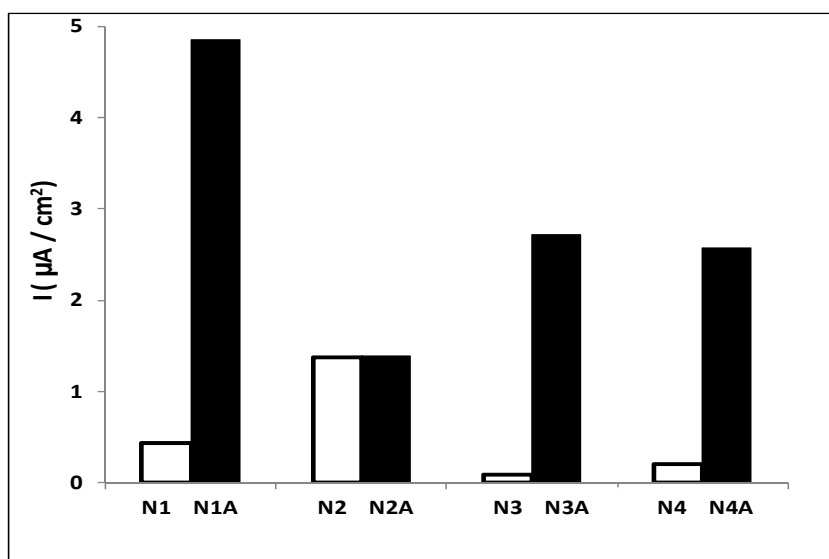


Figure 6: Photocurrent density of the bare Ni oxide and Ni/Al oxide films at 400 nm in 0.1M  $\text{Na}_2\text{SO}_4$ .

Finally, some preliminary results have been obtained when Ti/Al oxide electrodes were used as photo-anodes in PEC for the oxidation of glycerol (used as model organic compound). Such application could be also proposed for processes in which the presence of a hole scavenger is exploited to increase the global yield of the PEC. Experiments were done to verify the different response of the active sites at different pH. Table 2 resumes the values of photocurrent measured at 400 nm at T1A sample.

Table 2: Normalized photocurrents, derived from the data obtained at different electrolyte pH values, for the T1A sample ( $\lambda=400$  nm ; 0.5V of overpotential ).

Electrolyte	0.1 M KOH	0.1 M KNO <sub>3</sub>	0.1 M H <sub>2</sub> SO <sub>4</sub>
I <sub>T1A</sub> (mA / W)	3.53	0.86	0.53
Electrolyte	0.1 M KOH / 30 % Glycerol	0.1 M KNO <sub>3</sub> / 30% Glycerol	0.1 M H <sub>2</sub> SO <sub>4</sub> / 30 % Glycerol
I <sub>T1A</sub> (mA / W)	1.88	1.04	1.54

Data may give useful indications on the reaction mechanism. It is observed that the best performances are always obtained in basic solutions, either in the raw supporting electrolyte or in the presence of glycerol. A similar result could be expected when oxygen evolution reaction (OER) is the main process, as in the case of supporting electrolyte.

The still highest current measured in the presence of glycerol indicates that also its oxidation is favored in this medium. However, the decrease in the absolute value of the photocurrent at basic pH may indicate that a direct oxidation of glycerol is occurring at the electrode surface, which may compete with the most favored OER. At neutral and acidic pH, when OER is less favored, the presence of glycerol always increases the resulting photocurrent.

#### 4. Conclusions

The positive effect of embedding Al oxide into Ti and Ni nanostructured electrodes has been shown. The performances of the structures were tested in the near of the visible range of the light: the best results (among all the Ni/Al films) were obtained at N1A sample in which commercial nanopowders of NiO were combined with Al oxide. At this sample, a photocurrent value more than 11 times higher than that obtained at the bare NIO sample was recorded. Samples of Ti/Al oxides were also tested for the oxidation of glycerol: the results obtained at different pH gave indications on the reaction mechanism at the electrode surface.

#### Reference

- Castillo C.E., Sandroni M., Légalité F., Gennari.M, Stoll T., Fortage J., Blart E., Pellegrin Y., Delacote C., Rannou P., Sadki S., Boujita M., Deronzier A., Collomb M., Odobel F., 2015, Visible Light-Driven Electron Transfer from a Dye-Sensitized p-Type NiO Photocathode to a Molecular Catalyst in Solution: Toward NiO-Based Photoelectrochemical Devices for Solar Hydrogen Production, *J. Phys. Chem. C*, 119 (11), 5806–5818, DOI: 10.1021/jp511469f.
- D'Amario L., Boschloo G., Hagfeldt A., Hammarström L., 2014, Tuning of Conductivity and Density of States of NiO Mesoporous Films Used in p-Type DSSCs, *The journal of physical chemistry*, 118, 19556–19564.
- Hu C., Chu K., Zhao Y., Teoh W.Y., 2014, Efficient Photoelectrochemical Water Splitting over Anodized p-Type NiO Porous Films, *ACS Appl. Mater. Interfaces*, 6, 18558–18568.
- Li F., Zhao Y., Hao Y., Wang X., Liu R., Zhao D., Chen D., 2012, N-doped P25 TiO<sub>2</sub>-amorphous Al<sub>2</sub>O<sub>3</sub> composites: One-step solution combustion preparation and enhanced visible-light photocatalytic activity, *Journal of Hazardous Materials*, 239–240, 118–127.
- Li Y., Yu H., Zhang C., Fu L., Li G., Shao Z., Yi B., 2013, Electrodeposition of Ni oxide on TiO<sub>2</sub> nanotube arrays for enhancing visible light photoelectrochemical water splitting, *Journal of Electroanalytical Chemistry* 688, 228–231.
- Palmas S., Mascia M., Vacca A., Llanos J., Mena E., 2014, Analysis of photocurrent and capacitance at TiO<sub>2</sub> nanotubes/polyaniline hybrid composites synthesized through electroreduction of aryldiazonium salt, *RSC Advances*, 46, 23936-24419.
- Palomares E., N. Clifford J.N., Haque S.A., Lutz T., R. Durrant J.R., 2003, Control of charge Recombination Dynamics in Dye Sensitized Solar Cells by The use of Conformally Deposited Metal Oxide Blocking Layers, *J. AM. CHEM. SOC.*, 125, 475-482.